

Fingerprint Reconstruction: Approaches to Improve Fingerprint Images

Milind B Bhilavade^{1*}, Dr.K.S. Shivaprakasha², Dr. Meenakshi R. Patil³, and Dr. Lalita S Admuthe⁴

^{1*}Research Scholar, VTU, Belagavi, Assistant Professor, Department of Electrical Engineering, JJMCOE Jaysingpur, India. milind2006@gmail.com, <https://orcid.org/0009-0004-1146-1109>

²Professor, Department of ECE, N.M.A.M. Institute of Technology, NITTE (Deemed to be University), Nitte, India. shivaprakasha.ks@nitte.edu.in, <https://orcid.org/0000-0002-5078-6078>

³Professor, Department of Electronics Engineering, C M R Institute of Technology, Bengaluru, India. meenakshirpatil@gmail.com, <https://orcid.org/0000-0002-2225-5333>

⁴Professor, Department of Electronics Engineering, D K T E's College of Engineering, Ichalkaranji, India. ladmuthe@gmail.com, <https://orcid.org/0009-0005-6619-1772>

Received: September 04, 2023; Revised: November 11, 2023; Accepted: January 09, 2024; Published: March 30, 2024

Abstract

Fingerprint reconstruction methods have been initially proposed to spoof the fingerprint identification systems, wherein the fingerprints are generated from the fingerprint features stored in the database for template matching/identification purpose. The reconstructed fingerprints attempt to validate in the absence of the user/person. The poor fingerprint Images with scratches on fingerprint image or latent fingerprints or overlapping fingerprints shall also be reconstructed for personality identification. In this paper we discuss the two fingerprint reconstruction methods, one which uses minutiae features for reconstruction and the other one uses deep learning methods to reconstruct the fingerprint images. The poor fingerprint image which fails to validate the identity due to various reasons like poor skin condition/large cuts on the fingers/wet fingers/poor scanning of images shall be reconstructed for increasing the matching accuracy. The requirement of performance measure parameters used for evaluation of these systems are equal error rate, false acceptance rate, false rejection rate and average matching score. The deep learning methods are more suitable for reconstructing the fingerprint images that appear damaged due to poor skin condition/large cuts on the fingers/wet fingers/poor scanning of images. In terms of matching score comparison, the deep learning methods have matching scores in between 23-94% whereas for minutiae-based techniques the matching score is between 82 and 99.99%. The other performance parameter is the equal error rate (ERR) required to meet has to be closer to 0. The matching score is computed with the assumptions of false acceptance rate (FAR) ranging from 1% to 0%.

Keywords: Fingerprint, Ridge Reconstruction, Scratch, Finger Cuts.

1 Introduction

Electronic equipment and digital gadgets in use today widely utilize biometric features of users to assure the security of their devices. The very purpose of biometric is to check the authenticity of the user using the device. Advancement in technology proposes various methods of validation of authenticity. Biometric features used for user validation include face, iris, palm, fingerprints and hybrid systems with usage of face and fingerprint both. Whereas the verification systems with fingerprints of a user have been the first choice of the users over the conventional system. Cost effective fingerprint-based user validation systems are still more popular. Biometric features not only used for user authentication but also in use for personality verifications of various public schemes implemented by government organizations. The unique identification systems recognized by governments utilize hybrid systems for personality validations. It has been observed many times that the user/beneficiary has to go for multiple time registrations for accurate validation due to various reasons. Therefore, assuring the implementation of a precise biometric system has still remained as a challenging task for the researchers. Several researchers are working on improving these biometric based systems. Among all biometric features fingerprint based validating systems are popular and have challenges to prove the authenticity even during poor/damaged fingerprints. The poor fingerprint may be generated due to improper scanning or poor skin conditions of the users (Yang & Järvinen 2019).

Numerous advancements in fingerprint matching have been proposed by diverse scholars to overcome challenges such as impartial screening and the dormant state of fingerprint impressions. It has come to attention that this matching process falters when distinct blemishes emerge on the fingertip of the user whose authentication is sought. These blemishes may manifest as a consequence of minor incisions on the user's fingertip. It is noteworthy to mention that fine lines can materialize on digits during the winter season, resulting in blemishes on the fingerprint patterns. Furthermore, burns or damp fingers also contribute to the misidentification of fingerprints. To tackle these concerns, multiple researchers have introduced fingerprint reconstruction techniques. The proliferation of high-resolution sensors presently employed for fingerprint scanning and the escalating demand for biometric-based devices have compelled researchers to craft more precise and reliable fingerprint recognition apparatus. Over the past two decades, numerous fingerprint recognition systems have been proffered. In order to gain familiarity with the prevailing methodologies, a comprehensive exploration of various fingerprint recognition systems has been undertaken in the course of this research endeavor. Fingerprint recognition will be executed in accordance with the utilization guidelines outlined in references (Park, C.H., 2004) (Jain, A.K., 2006) (Sheng, W., 2007) (Arora, S.S., 2014) (Yin, X., 2019) (Agrawal, P., 2014). Predominant fingerprint recognition systems predominantly rely on minutiae characteristics (Park, C.H., 2004) (Jain, A.K., 2006) (Sheng, W., 2007). Minutiae, encompassing ridge bifurcations, endpoints, hooks, eye-like patterns, and delta points as depicted in Figure 1, constitute the focal elements. Achieving level 3 attributes (Jain, A.K., 2006) mandates the employment of high-resolution scanners. While the fingerprint image displayed in Figure 1 was not acquired via a high-resolution scanner, it serves as a valuable reference for comprehending and scrutinizing the myriad minutiae elements pertinent to matching. Notably, the features exhibited in the illustration correspond to both level 1 and level 2 attributes (Jain, A.K., 2006) within the fingerprint domain. The ridge represents the broader line feature within a fingerprint image, while the valley delineates the recessed space separating two ridges. A ridge bifurcation denotes the point where a ridge diverges into two branches. In the midst of valleys, one may discern line fragments. Additionally, patterns resembling eyes and hooks are categorized as level 2 features (Jain, A.K., 2006).

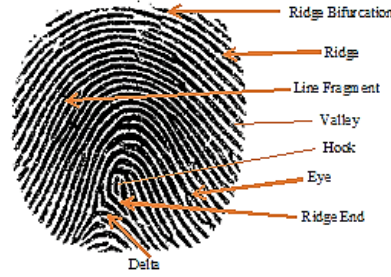


Figure 1: Level 1 and Level 2 Features of Fingerprint

The majority of fingerprint matching systems predominantly employ level 1 and level 2 characteristics for recognition due to their cost-effectiveness (Chen, C., 2016). However, it has come to the attention of many users that their identity may not be verified when their finger's skin condition is poor, such as having significant cuts or scars. To address this vulnerability in authentication, researchers have been proposing techniques for fingerprint reconstruction. Fingerprint image reconstruction methods have also been suggested to generate fingerprint images from their minutiae features, facilitating both Type-I and Type-II attacks. In a Type-I attack, the reconstructed fingerprint is matched with the original fingerprint to establish authenticity in the absence of the user, while in a Type-II attack, the reconstructed fingerprint is compared against different impressions of the original fingerprint (Chen, F., 2009). This paper's objective is to explore and assess various approaches to fingerprint reconstruction. The subsequent sections of this paper are structured as follows: Section II provides an overview of the current landscape of fingerprint reconstruction methods based on minutiae. The detailed discussion of the modern methods which use the intelligent approaches for reconstruction is presented in section III. Section IV highlights the comparison and analysis of these methodologies. Section V concludes the paper.

2 Reconstruction of Fingerprints from Minutiae Features

The approach of reconstructing the fingerprint Image from its minutiae features is described in this section which was basically proposed for masquerade attack (Ross, A.A., 2005) (Cappelli, R., 2007) (Chen, F., 2009) (Feng, J., 2010) (Cao, K., 2014) (Gupta, R., 2020) (Li, S., 2012). Majority of user authentication systems based on fingerprint use level 1 and level 2 minutiae features and stores these as the templates instead using fingerprint image. Therefore, the templates of these systems stored in the database contain these features and authentication is based on matching performance of these parameters. The researchers have tried to generate the fingerprint image from minutiae features stored in the template and generated fake fingerprints to infer the authentication process. This section of this paper elaborates on these methodologies.

Reconstruction of fingerprints from minutiae points (Ross, A.A., 2005) proposed by Ross et al concentrated on estimating the orientation map of corresponding fingerprints. The approach uses the gabor-like filter SFINGE (Ross, A.A., 2005). The cosine plane wave which is modulated using gaussian function is used as a filter f in equation (1).

$$f(v) = \frac{1}{\sigma^2} e^{-\frac{\|v\|^2}{2\sigma^2}} \left[\cos(k, v) - e^{-\frac{\sigma\|k\|^2}{2}} \right] \quad (1)$$

σ the variance is considered as 1.2 by the authors (Ross, A.A., 2005). The filter is applied at a point P in the image. The authors have proposed an algorithm for orientation estimation at any point P. They

have generated triplets by forming the triangles of three minutiae points. To estimate the orientation at point P(x,y) in any triplet is computed using equation (2).

$$\theta(x, y) = \frac{d_3}{d_1+d_2+d_3}\theta_1 + \frac{d_2}{d_1+d_2+d_3}\theta_2 + \frac{d_1}{d_1+d_2+d_3}\theta_3 \quad (2)$$

where θ_1 is the nearest orientation of the vertex to pixel P and θ_3 is the farthest orientation of the vertex to pixel P. The observed estimation of orientation is good for the larger size of triplets to recover the classes like whorl tented arch and loops. These classes have different minutiae in small areas. The vector $k=[k_x,k_y]$ shall be obtained from related frequency of filter $\frac{1}{\sigma}$ and estimated orientation θ by solving equation (3) and equation (4).

$$\frac{1}{\sigma} = \sqrt{k_x^2 + k_y^2} \quad (3)$$

$$\tan(\theta) = -\frac{k_x}{k_y} \quad (4)$$

The related frequency is kept the same for recovery of the entire image for the consideration of the same inter-ridge spacing. The result of reconstruction observed by authors is shown in figure 2. Though the reconstruction does not seem to be realistic it leads to note here that the fingerprint image can be reconstructed from minutiae points. To improve the efficacy of masquerade attack Raffaele et al proposed an approach to reconstruct fingerprint image from standard templates. The standard database templates (Cappelli, R., 2007) contain the record header and the number of fingerprint images acquired for one user. Record header (Cappelli, R., 2007) has the information related to image size. Each minutiae contains a 6-byte information corresponding to minutiae type, position, minutiae direction and minutiae quality (Cappelli, R., 2007). The additional information for matching purposes related to each view stored contains extended data record (Cappelli, R., 2007). Extended data record relates the data format which may include ridge count data or core and delta data format or zonal data (Cappelli, R., 2007). The authors have utilized the subsequent data attributes for the regeneration of the fingerprint picture: a) Vertical and Horizontal Image. Dimensions b) Image Clarity, which is reasonably assumed to possess equivalent horizontal and vertical clarity c) Quantity of Minutiae denoted as 'n' d) Attributes of each minutiae, encompassing their Type, Position 'x' and 'y', and Direction e) Core and Delta coordinates (Cappelli, R., 2007). The restorative methodology expounded in (Cappelli, R., 2007) commences with the utilization of template data to deduce multiple facets of the fingerprint (Fig. 3), including its overall size, image orientation, and ridge configuration. To imbue the fingerprint image with heightened realism, a rendering stage is executed. Forecasts concerning the fingerprint's dimensions factor in parameters labeled as 'a1', 'a2', 'b1', 'b2', and 'c', defining the fingerprint's shape, as depicted in figure 4.

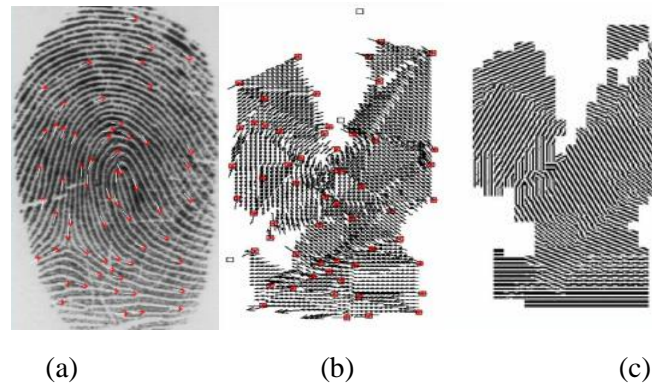


Figure 2: Courtesy (Ross, A.A., 2005) (a) Minutiae Distribution of a Fingerprint Image. (b) Predicted Orientation Map (c) Reconstructed Fingerprint

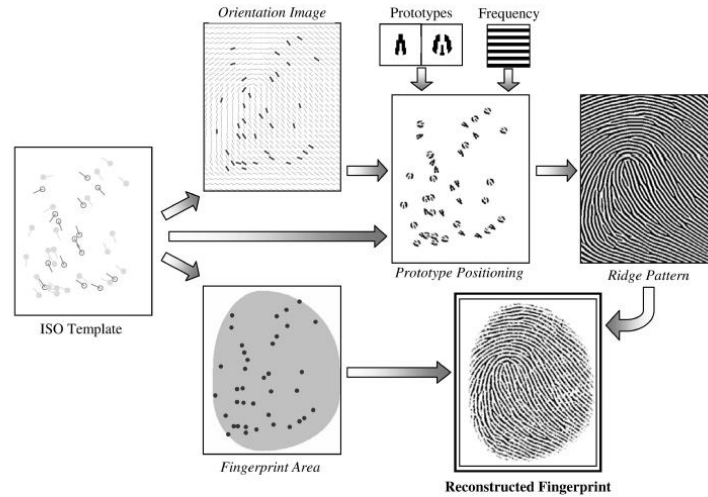


Figure 3: Fingerprint Reconstruction Approach Raffaele et al (Cappelli, R., 2007)

Though the reconstructed fingerprint image shown in figure 3 looks more realistic and contains all original minutiae, it also adds in a few extra minutiae points. To improve the Minutiae matching accuracy Chen et al (Chen, F., 2009) proposed an algorithm to produce the virtual minutiae using interpolation method and then used the virtual and real minutiae to reconstruct the orientation field. To improve the fingerprint matching score the orientation field matching score and minutiae matching score are combined using Neyman–Pearson rule (Chen, F., 2009). This paper the authors have concentrated on reconstructing the orientation field in the area (Sparse) where there are few minutiae points. Three minutiae points are selected in the sparse area and orientation field is first estimated in this area. Then the fingerprint image is divided into several triangles by adding the diagonal points from one to all other points. At any point in the triangle the virtual minutiae are located by computing the Euclidean distance from each of the vertices. Refer (Chen, F., 2009) to place the virtual minutiae based on orientation field estimation taking into consideration the Euclidean distance from each vertex. From real minutiae and virtual minutiae, the orientation field is reconstructed using polynomial model (Chen, F., 2009). The matching performance is increased by fusing the orientation field matching score with minutiae matching score using Neyman–Pearson rule (Chen, F., 2009). However, the computational cost increases due to the use of fusion algorithms.

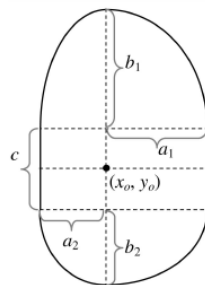


Figure 4: Parameters for Fingerprint Image Estimation (Cappelli, R., 2007)

Selected in the sparse area and orientation field is first estimated in this area. Then the fingerprint image is divided into several triangles by adding the diagonal points from one to all other points. At any point in the triangle the virtual minutiae is located by computing the Euclidean distance from each of the vertices. Refer (Chen, F., 2009) to place the virtual minutiae based on orientation field estimation taking into consideration the Euclidean distance from each vertex. From real minutiae and virtual

minutiae the orientation field is reconstructed using polynomial model (Chen, F., 2009). The matching performance is increased by fusing the orientation field matching score with minutiae matching score using Neyman–Pearson rule (Chen, F., 2009). However, the computational cost increases due to the use of fusion algorithms.

Feng and Jain (Feng, J., 2010) introduce a novel approach for fingerprint regeneration, transitioning from minutiae data to phase information. Within a 9x9 pixel sub-block, an innovative alteration for the central pixel is recommended, facilitating the prediction of an orientation value for each block. This is achieved by consulting the nearest minutiae points within each of the eight designated sectors. In contrast, Cao and Jain (Cao, K., 2014) present an alternative method for fingerprint reconstruction, which entails transforming minutiae data into a complete fingerprint image. This technique leverages pre-existing knowledge of ridge patterns, effectively employing an orientation patch dictionary to regenerate the orientation field. Both these methods use the AM-FM model to reconstruct the ridge pattern. In the AM-FM model (Feng, J., 2010) (Cao, K., 2014) a 2D fingerprint image shall be represented by amplitude and frequency modulated signal $I(x,y)$ (5).

$$I(x,y) = a(x,y) + b(x,y) \cdot \cos(\psi(x,y)) + n(x,y) \quad (5)$$

This equation consists four components i) $a(x,y)$: Intensity component ii) $b(x,y)$: amplitude component iii) $\psi(x,y)$: Phase component iv) $n(x,y)$: noise component. A phase component $\psi(x,y)$ can be decomposed into two parts (Feng, J., 2010) (Cao, K., 2014): continuous phase $\psi_c(x,y)$ and spiral phase $\psi_s(x,y)$ with

$$\psi_c(x,y) = \sqrt{x^2 + y^2} \quad (6)$$

$$\psi_s(x,y) = \sum_{j=1}^n p_j \tan^{-1} \left(\frac{y-y_j}{x-x_j} \right) \quad (7)$$

Where $p_j \in \{-1,1\}$ denoting the polarity for positive and negative spirals.

Feng and Jain (Feng, J., 2010) estimated the FM representation of fingerprint in four steps to obtain $\psi(x,y)$. In the first step they have proposed to estimate the orientation field with/without given singular points. In their second step they estimated the gradient of the continuous phase. To avoid discontinuity in phase gradient they have adopted branch cut phase unwrapping (refer (Feng, J., 2010)) algorithm to compute unwrapped orientation field. To map the ridge orientation and frequency the gradient of continuous phase is computed by interpolation. In the next step the continuous phase is reconstructed using a piecewise planer model. The phase offset for the block (m,n) of 8 X 8 pixels at every border pixel (x,y) is estimated using the equation (8)

$$\psi = G_{cx}(m-1,n)x + G_{cy}(m-1,n)y + P(m-1,n) - G_{cx}(m,n)x - G_{cy}(m,n)y \quad (8)$$

$G_{cx}(m,n)$ and $G_{cy}(m,n)$ are the two components of gradient continuous phase $G_c(m,n)$. Then $P(m,n)$ is phase offset which is estimated as the mean value of the offsets estimated by (8). Finally, the fingerprint image is obtained by combination of Phase spiral and continuous phase. The reconstructed image still contains the false/ spurious minutiae in the singularity region.

A dictionary-based fingerprint reconstruction method is proposed by Cao and Jain (Cao, K., 2014). This method reconstructs the fingerprint Image from minutiae. The method considers the prior knowledge of ridge structure as an orientation patch dictionary and reconstructs the orientation field. Whereas to reconstruct the ridge pattern the continuous phase dictionary is used. The few spurious minutiae generated during this estimation are removed using the AM-FM model. Though this model has increased the matching accuracy from the reconstructed fingerprint it does not look like a realistic fingerprint image and anyone can identify that this is a generated to fool the human experts' sets. Gupta et al. (Gupta, R., 2020) have presented a comparable methodology for reconstructing fingerprint images,

focusing on minutiae density and the orientation field's direction to restore the orientation and phase of the fingerprint image. In contrast, Li and Kot (Li, S., 2012) have introduced an enhanced approach for the comprehensive reconstruction of fingerprint images. Their technique employs the AM-FM model to restore the continuous phase, eliminating spirals derived from the phase image, initially estimated from the ridge pattern. To mitigate artifacts stemming from phase discontinuities, they have incorporated a refinement procedure for the reconstructed phase image, merging the continuous phase with the spiral phase. Ultimately, this refined phase image serves as the foundation for generating a thinned version of the fingerprint, subsequently used to craft a realistic grayscale fingerprint image. As mentioned in the beginning of this section all these efforts are made to fool the human experts by estimating a fingerprint image which looks similar to the original one. This has created a challenge to the researchers working in developing the authentication systems which use fingerprint matching technologies based on minutiae points.

3 Fingerprint Reconstructions Using Neural Networks

In this section we discuss the usage of neural networks in fingerprint recognition and reconstruction. Network in network (NIN) structure (M. Lin, 2014) had been proposed to enhance the discrimination modality of images for the patches that fall within the field of reception. The authors have demonstrated that the NIN structures perform better for object detections. Convolution Neural networks consist of sequences of layers. Each layer transforms one set of data to another through a differentiable function; a simple convolution layer is shown in Fig 5 a. The multilayer micro network structure implemented and tested by Lin et al (M. Lin, 2014) is shown in fig 5.b. The first layer of fig 5 b is compatible with the convolution layer shown in fig 5 a whereas the next layer has cross channel parametric pooling structure which allows complex and learnable cross channel information. Multiple cross channel layers shall be cascaded to increase the complexity and better training of the network (Arora 2024).

Nesreen et al (Alsharman, N., 2022) proposed to use convolutional neural network (CNN) architecture for fingerprint classification into three main categories i.e., arch, loop, and whorl. The cascaded structure of multiple convolutional layers used for categorization is shown in fig 6. After classification, fingerprint matching performance is improved for the bifurcation minutiae extraction-based fingerprint matching algorithm. The categorization made by authors is based on a pattern mathematical model using GoogleNet, AlexNet, and ResNet Convolutional Neural Network (CNN) architecture. Where 70% of their data is used for training purposes and that of 30% is used for testing. Kanishka et al (Wijewardena, K.P., 2022) assessed a performance of deep learning-based fingerprint invertibility method implemented for reconstruction using minutiae features and deep networks. This indicates that the deep learning methods enabled better fingerprint recognition and better fingerprint invertibility. Fingerprint invertibility method refers to creating a fingerprint image from its feature templates stored for fingerprint recognition.

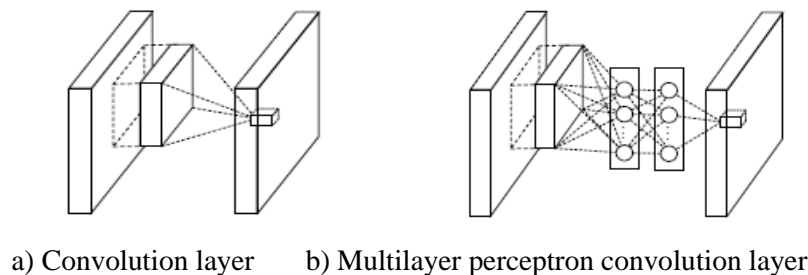


Figure 5: Structures of Convolution Layers (M. Lin, 2014)

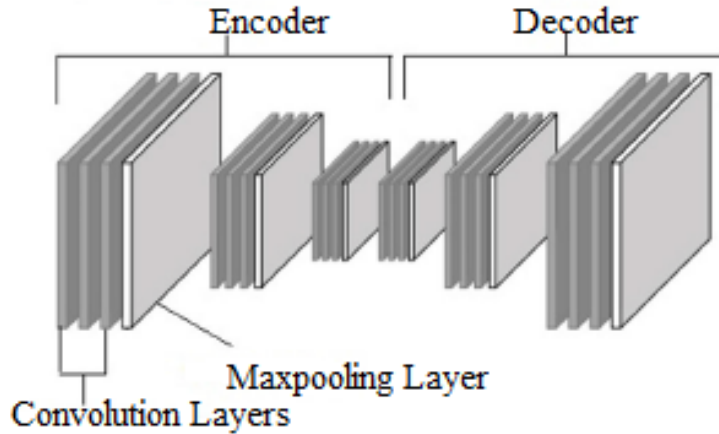


Figure 6: Structure of CNN Autoencoder

Saponara and colleagues (Saponara, S., 2021) employed Convolutional Neural Network (CNN) autoencoders to regenerate fingerprint images. Autoencoder models exhibit a unique capacity for autonomously replicating their own inputs during the training process, harnessing self-learning layers to extract fingerprint features while simultaneously reducing dimensions. The conventional architecture of a CNN autoencoder comprises a series of cascading convolutional layers, as depicted in Figure 6. Convolutional autoencoders utilize convolution operators to encode input characteristics and accurately reproduce them in the output while minimizing reconstruction errors. Consequently, this autoencoder encompasses both encoder and decoder components, ensuring that input and output dimensions remain unchanged, simplifying the comparison between the reconstructed output and the original input. The k th feature map in the encoder is computed with equation 9.

$$h^k \sigma (x \star W^k + b^k) \quad (9)$$

Where σ is an activation function and \star is a convolutional operator for two-dimensional data. The decoder part reconstructs the data using equation (10).

$$y = \sigma (\sum_{k \in H} (h^k \star \tilde{W}^k) + c) \quad (10)$$

In this equation (10) H represents the feature space and c is the bias parameter for the input channel. 11 convolutional layers are used to map the feature space in the algorithm implemented by Saponara et al (Saponara, S., 2021). Maxpooling layers used in the auto encoder reduces the image size by down sampling the input image into smaller images/regions. The CNN auto encoders sharpen the reconstructed images with increased amount of identification accuracy ranging from 95% to 98.7%. The MSE between the input and output images is observed from 0.0013 to 0.0048.

Deep learning methods are also used to separate and enhance the latent fingerprint images (Liu, M., 2020) and overlapped fingerprint images (Yoo, D., 2020). Generative adversarial Networks (GAN) for data synthesis and reconstruction of latent fingerprints (Xu, Y., 2020). GAN is also used for improving synthesis and reconstruction of fingerprints to improve the ability to spoof the fingerprint validation systems. The deep learning methods shall be used to reconstruct the poor fingerprint images to improve the fingerprint validation systems (Ding, B., 2020) (Attia, M., 2019) (Xin, R., 2020) (Kauba, C., 2021).

4 Performance Measures Used for Fingerprints Reconstruction Methods

To evaluate the performance of fingerprint reconstruction methods most of the researchers compute the average matching score. Successful matching score is computed based on the ratio of the number of successful matches registered to the total number of attempts made to match the reconstructed fingerprints with the templates in the database. The required score should be closer to 1 or 100%. The other measuring parameter used by researchers is equal error rate (ERR) obtained from false acceptance ratio (FAR) and false rejection ratio (FRR).

$$FAR = \frac{\text{Number of False acceptances}}{\text{Total Number of acceptances}} \quad (11)$$

$$FRR = \frac{\text{Number of False Rejections}}{\text{Total Number of identification attempts}} \quad (12)$$

The Equal Error Rate (EER) stands as a customary performance metric utilized for benchmarking and contrasts. EER designates the juncture where the False Acceptance Rate (FAR) and the False Rejection Rate (FRR) intersect. A more commendable system is indicated by a diminished EER value (Ross, A.A., 2005). Yet, it's an unattainable feat to achieve a 0% EER using biometric methods (Cappelli, R., 2007). The true acceptance rate (TAR) or identification rate shall be evaluated as a performance measuring metric with the consideration of different values of FAR. The TAR is computed based on the number of successful matching acceptance (identifications) against the total number of attempts made for acceptance. Various fingerprint reconstruction methods have been proposed in literature and are compared in table 1. From the table it is clear that the researchers have achieved a TAR up 99.9% for reconstruction of fingerprints from Minutiae. These minutiae-based systems basically proposed to spoof the fingerprint authentication methods. The methods implemented using deep networks or CNN based fingerprint reconstruction methods have been suggested to provide security of authentication in the absence of authentic user. The fingerprint images are reconstructed from the features of the image which are appeared poor while scanning or damaged by some reasons.

5 Conclusion

There are various approaches to fingerprint image reconstruction. Reconstruction from minutiae features has been proposed for spoofing the matching systems. The comparison illustrated in Table 1 indicates that the fingerprint reconstruction methods-based AM_FM model has ERR very close to 0 with average matching score of 95 % to 99%. Though the matching score of deep learning-based methods are not good and are from 20% to 89% these methods are secure against Type-I and Type-II attacks. Basically, the AM-FM based models are implemented to fool the fingerprint identification system and generate spurious/false minutiae points. Deep learning methods show satisfactory matching score and are useful in fingerprint reconstruction for damaged fingerprint images and also more secure against type-I and Type-II attacks. Our research will focus on developing the deep learning-based algorithm to reconstruct the poor/damaged fingerprint images for more matching accuracy resilient to type-I and Type-II attacks.

Table 1: Comparison of Various Fingerprint Reconstruction Approaches

Sr. No.	Algorithm	Type of Fingerprint reconstruction	Performance Evaluation	Comments
1	Ross et al	Reconstruction of Ridge from Minutiae triplets	82% of true classification rate was achieved. 22% images of each class are used for training and 78% Images are used for testing	Nist-4 database of 2000 Images.
2	Cappelli et al	Reconstruction of ridge pattern using Gabor filter	Different security levels in terms of False matching rate (FMR) are considered for performance measure. The average percentage of successful attacks was 81 percent at a high security level and 90 percent at a medium security level.	FVC 2002 database 1 is used
3	Chen et al	The reconstruction of the orientation field entails the utilization of both virtual and actual minutiae. The process involves employing both an interpolation technique and a model-based approach to regenerate the orientation field.	Type 1 attack 81.9% TAR at 0% FAR for FVC2002 DB1. FAR and FRR are minimized by using fusion scheme.	FVC2002 DB1, DB2 and the THU database are used.
4	Feng et al	The orientation field is reconstituted through the application of the FM model. To achieve a reconstructed fingerprint, the process involves the reconstruction of the orientation field, the restoration of the continuous phase, and the amalgamation of this continuous phase with the spiral phase.	Type 1 attack 94.13% TAR at 0% FAR for FVC2002 DB1. 99.7% rank-1 identification for NIST SD4; Type-2 Attack: 45.89% TAR at 0% FAR for FVC2002 DB1. 65.75% rank-1 identification for NIST SD4;	The fingerprint verification was performed on FVC2002 DB1 and Fingerprint identification experiment was performed on NIST SD4
5	Cao et al	Orientation field is reconstructed from orientation field patch and ridge pattern is reconstructed using continuous phase patch dictionary.	Type 1 attack 100% TAR at 0.01% FAR for FVC2002 DB1 and FVC2002 DB2. 100% rank-1 identification for NIST SD4; Type-2 Attack: 85.23% and 90.29% TAR at 0.01% FAR for FVC2002 DB1 and FVC2002DB2 respectively. 80.55% rank-1 identification for NIST SD4;	The fingerprint verification was performed on FVC2002 DB1 and FVC2002 DB2 Fingerprint identification experiment was performed on NIST SD4
6	Gupta et al	Nearest minutiae in eight sectors, continuous phase generation, AM-FM model for correction	Type 1 attack: 97.95% TAR for FVC2002 and 94.09% for FVC2004 Type 2 attack: 49.25% and 50.02% TAR for FVC 2002 and FVC2004	FVC 2002 and FVC 2004 database is used verification and identification. Reduces minutiae.
7	Li et al	Full fingerprint image reconstruction based on AM-FM model. Artifacts due to the discontinuity in the continuous phase are reduced by a refinement Process applied on reconstructed image.	Type I attack: 86.48% and 70.25% TAR at 0.01% FAR for FVC2002 DB1 Set I and Set II. 86.96% and 68.96% TAR at 0.01% FAR for FVC2002 DB2 Set I and Set II.	FVC 2002 DB1 Set I and Set-II are used for experimentation.
8	Kanishka et al	Fingerprint reconstruction using Deep fingerprint templates	Type 1 attack 85.95% TAR at 0.01% FAR identification for NIST SD4; Type-2 Attack: 68.1% TAR at 0.01% FAR for NIST SD4;	Matching performance is reduced whereas more resistant to reconstruction attacks.
9	Sergio et al	CNN auto encoders are used to reconstruct the fingerprint images	Identification rate of reconstructed fingerprints images is 98.1%, 97%, 95.9%, and 95.02% for FVC2004 Dataset I, Dataset II, Dataset III, Dataset IV respectively.	The input image features are extracted and replicated in a well-defined manner in the output image.
10	Liu et al	Latent fingerprints are reconstructed using deep nested UNets	Identification rate of reconstructed fingerprints images is 20%, and 22% for NIST SD27 and IIITD-MOLF latent fingerprint databases respectively.	NIST SD27 and IIITD-MOLF latent fingerprint databases are used.
11	Yoo et al	Overlapped latent fingerprints are reconstructed using Finsnet CNN	75.5% TAR at 0.001% FAR identification for Tsinghua OLF database and 84.5% TAR at 0.001% FAR identification for Tsinghua SOF database.	Tsinghua SOF database is created by overlapping FVC2002 database images
12	Ying et al	To improve latent fingerprint reconstruction GAN based data augmentation scheme is used	Identification rate of reconstructed fingerprints images is 69.38% to 81.1% for NIST SD27 with different rank and 86.86% to 94.43% for IIITD-MOLF latent fingerprint databases respectively.	NIST SD27 and IIITD-MOLF latent fingerprint databases are used
13	Rafael et al	StyleGan2 architecture is used for synthesis and reconstruction of Fingerprints.	Type 1 attack: 99.92% TAR at 1% FAR, 99.67% TAR at 0.1% FAR, 99.26% TAR at 0.01% FAR and 99.23 % TAR at 0% FAR for NIST SD4 Type 2 attack: 97.67% TAR at 1% FAR, 93.67% TAR at 0.1% FAR, 86.32% TAR at 0.01% FAR and 85.44 % TAR at 0% FAR for NIST SD4	NIST SD14 used for fingerprint matching and classification. NIST SD4 dataset is used for assessing performance of synthesis and reconstruction

References

- [1] Agrawal, P., Kapoor, R., & Agrawal, S. (2014). A hybrid partial fingerprint matching algorithm for estimation of equal error rate. In *IEEE International Conference on Advanced Communications, Control and Computing Technologies*, 1295-1299.
- [2] Alsharman, N., Saaidah, A., Almomani, O., Jawarneh, I., & Al-Qaisi, L. (2022). Pattern Mathematical Model for Fingerprint Security Using Bifurcation Minutiae Extraction and Neural Network Feature Selection. *Security and Communication Networks*, 1-16.
- [3] Arora, G. (2024). Desing of VLSI Architecture for a flexible testbed of Artificial Neural Network for training and testing on FPGA. *Journal of VLSI Circuits and Systems*, 6(1), 30-35.
- [4] Arora, S.S., Liu, E., Cao, K., & Jain, A.K. (2014). Latent fingerprint matching: performance gain via feedback from exemplar prints. *IEEE Transactions on Pattern Analysis and Machine Intelligence*, 36(12), 2452-2465.
- [5] Attia, M., Attia, M.H., Iskander, J., Saleh, K., Nahavandi, D., Abobakr, A., & Nahavandi, S. (2019). Fingerprint synthesis via latent space representation. In *IEEE International Conference on Systems, Man and Cybernetics (SMC)*, 1855-1861.
- [6] Bouzaglo, R., & Keller, Y. (2022). Synthesis and reconstruction of fingerprints using generative adversarial networks, 1-9.
- [7] Cao, K., & Jain, A.K. (2014). Learning fingerprint reconstruction: From minutiae to image. *IEEE Transactions on information forensics and security*, 10(1), 104-117.
- [8] Cappelli, R., Maio, D., Lumini, A., & Maltoni, D. (2007). Fingerprint image reconstruction from standard templates. *IEEE transactions on pattern analysis and machine intelligence*, 29(9), 1489-1503.
- [9] Chen, C., Anada, H., Kawamoto, J., & Sakurai, K. (2016). A hybrid encryption scheme with key-cloning protection: user/terminal double authentication via attributes and fingerprints. *Journal of Internet Services and Information Security*, 6(2), 23-36.
- [10] Chen, F., Zhou, J., & Yang, C. (2009). Reconstructing orientation field from fingerprint minutiae to improve minutiae-matching accuracy. *IEEE Transactions on image processing*, 18(7), 1665-1670.
- [11] Ding, B., Wang, H., Chen, P., Zhang, Y., Guo, Z., Feng, J., & Liang, R. (2020). Surface and internal fingerprint reconstruction from optical coherence tomography through convolutional neural network. *IEEE Transactions on Information Forensics and Security*, 16, 685-700.
- [12] Feng, J., & Jain, A.K. (2010). Fingerprint reconstruction: from minutiae to phase. *IEEE transactions on pattern analysis and machine intelligence*, 33(2), 209-223.
- [13] Gupta, R., Khari, M., Gupta, D., & Crespo, R.G. (2020). Fingerprint image enhancement and reconstruction using the orientation and phase reconstruction. *Information Sciences*, 530, 201-218.
- [14] Jain, A.K., Chen, Y., & Demirkus, M. (2006). Pores and ridges: High-resolution fingerprint matching using level 3 features. *IEEE transactions on pattern analysis and machine intelligence*, 29(1), 15-27.
- [15] Kauba, C., Kirchgasser, S., Mirjalili, V., Uhl, A., & Ross, A. (2021). Inverse biometrics: Generating vascular images from binary templates. *IEEE Transactions on Biometrics, Behavior, and Identity Science*, 3(4), 464-478.
- [16] Li, S., & Kot, A.C. (2012). An improved scheme for full fingerprint reconstruction. *IEEE Transactions on Information Forensics and Security*, 7(6), 1906-1912.
- [17] Liu, M., & Qian, P. (2020). Automatic segmentation and enhancement of latent fingerprints using deep nested unets. *IEEE Transactions on Information Forensics and Security*, 16, 1709-1719.
- [18] M. Lin, Q. Chen, and S. Yan (2014). Network in Network. <https://doi.org/10.48550/arXiv.1312.4400>

- [19] Park, C.H., Lee, J.J., Smith, M.J., Park, S.I., & Park, K.H. (2004). Directional filter bank-based fingerprint feature extraction and matching. *IEEE Transactions on Circuits and Systems for Video Technology*, 14(1), 74-85.
- [20] Ross, A.A., Shah, J., & Jain, A.K. (2005). Toward reconstructing fingerprints from minutiae points. *In Biometric Technology for Human Identification II*, 5779, 68-80.
- [21] Saponara, S., Elhanashi, A., & Zheng, Q. (2021). Recreating fingerprint images by convolutional neural network autoencoder architecture. *IEEE Access*, 9, 147888-147899.
- [22] Sheng, W., Howells, G., Fairhurst, M., & Deravi, F. (2007). A memetic fingerprint matching algorithm. *IEEE Transactions on Information Forensics and Security*, 2(3), 402-412.
- [23] Wijewardena, K.P., Grosz, S.A., Cao, K., & Jain, A.K. (2022). Fingerprint template invertibility: Minutiae vs. deep templates. *IEEE Transactions on Information Forensics and Security*, 18, 744-757.
- [24] Xin, R., Zhang, J., & Shao, Y. (2020). Complex network classification with convolutional neural network. *Tsinghua Science and technology*, 25(4), 447-457.
- [25] Xu, Y., Wang, Y., Liang, J., & Jiang, Y. (2020). Augmentation data synthesis via gans: Boosting latent fingerprint reconstruction. *In ICASSP IEEE International Conference on Acoustics, Speech and Signal Processing (ICASSP)*, 2932-2936.
- [26] Yang, Z., & Järvinen, K. (2019). Towards Modeling Privacy in WiFi Fingerprinting Indoor Localization and its Application. *Journal of Wireless Mobile Networks, Ubiquitous Computing, and Dependable Applications*, 10(1), 4-22.
- [27] Yin, X., Zhu, Y., & Hu, J. (2019). 3D fingerprint recognition based on ridge-valley-guided 3D reconstruction and 3D topology polymer feature extraction. *IEEE transactions on pattern analysis and machine intelligence*, 43(3), 1085-1091.
- [28] Yoo, D., Cho, J., Lee, J., Chae, M., Lee, B., & Lee, B. (2020). Fins Net: end-to-end separation of overlapped fingerprints using deep learning. *IEEE Access*, 8, 209020-209029.

Authors Biography



Milind B Bhilavade, received his Diploma in Electrical Engineering from WCE Sangli in 1998. Completed BE (Instrumentation Engineering) and ME in Control systems from Shivaji University Kolhapur in 2001 and 2008 respectively. Presently he is research student of VTU Belagavi Karnataka state India. Authors research area includes Image processing and Digital Image Inpainting. The author has worked as Lecture BCE Shravanbelgola Karnataka state India from 2003 to 2007. Presently he is working as assistant professor in JJMCOE Jaysingpur, Maharashtra from 2007. Mr. Bhilavade is life member of ISTE from 2009.



Dr.K.S. Shivaprakasha, received his B.E. (Electronics & Communication) degree from Bahubali College of Engineering, Visvesvaraya Technological University, Karnataka with IX rank in the university and M.Tech. (Digital Electronics and Communication Systems) degree from Malnad College of Engineering, Visvesvaraya Technological University, Karnataka with I rank with Gold Medal in the university in 2004 and 2007, respectively. Author completed his Ph.D. from National Institute of Technology Karnataka (NITK), Surathkal, Karnataka, in the field of Wireless Sensor Networks in 2015. Authors areas of research interest include Wireless Sensor Networks, Mobile Adhoc Networks, Information Coding Theory and Cryptography Currently, he is an Associate Professor in the Department of Electronics and Communication Engineering, N.M.A.M. Institute of Technology, Nitte, Karnataka. He has published more than 20 papers in reputed international/national journals and conferences and has co-authored a book on "Information Theory and Coding" for Wiley (India) publications.



Dr. Meenakshi R. Patil (M-07, SM-17) became member IEEE in 2007 and senior member of IEEE in 2017. Author is graduated in Electronics and Communication Engineering from PVPIT Budhagaon in 1994 and received post graduate degree in Electronics Engineering from WCE Sangli in 2002. Author has completed her Phd degree from Shivaji University Kolhapur in 2011. Authors research interest includes digital watermarking, Digital Image processing, Communication and network security. From 1999 to 2007, she was a head of department BCE Shraavanbelgola. Since 2011, she has been Professor with the AGM Group of institutions Hubballi, Karanataka state India. She is worked with JAGMIT Jamkhandi, Karnataka state India up to September 2020. Presently she is working as professor in E&CE Department, CMRIT, Bangluru from October 2021. Presently five research students are working on various fields in Signal processing and communication under her supervision Dr. Patil is life member of ISTE since 2002. Dr. Patil has designed a digital trainer kit which they are using it in their laboratories for education purpose.



Dr. Lalita S Admuthe, (M'15) member of IEEE, Computer Society. Author has received the M.E. and PhD. Degree in electronics engineering both from Shivaji University Kolhapur, India in 1994 and 2013 respectively. Authors research interest includes Neural Networks, Wireless Networks, Fuzzy Logic and Optimization Problems. Since 2013 she has been a Professor in Electronics Engineering at DKTE's Textile and Engineering Institute Ichalkaranji. Currently she is working as Director and Head of Electronics Engineering Department in the same institute. Her teaching experience includes the topics of Artificial Neural Networks, Radom Signal Processing, Computer Architecture and Parallel Processing.